Cell

Cohesin Complex Promotes Transcriptional Termination between Convergent Genes in *S. pombe*

Monika Gullerova[1] and Nick J. Proudfoot[1,*]
[1]Sir William Dunn School of Pathology, University of Oxford, South Parks Rd, Oxford OX1 3RE, UK
*Correspondence: nicholas.proudfoot@path.ox.ac.uk
DOI 10.1016/j.cell.2008.02.040

SUMMARY

Transcription analyses reported in these studies reveal that convergent genes in *S. pombe* generate overlapping transcripts in the G1 phase of the cell cycle. We show that this double-strand (ds) RNA induces localized RNAi (Dicer and RITS) dependent transient heterochromatin structures including histone H3 lysine 9 trimethylation marks and Swi6 association. Consequently cohesin is recruited to these chromosomal positions through interaction with Swi6. In G2, localized cohesin is further concentrated into the intergenic regions of the convergent genes tested. This results in a block to further dsRNA formation by promoting gene-proximal transcription termination between the convergent genes. Cohesin release at mitosis leads to a new G1 phase with repeated dsRNA formation, transient heterochromatin, and cohesin recruitment. Our results uncover a hitherto unanticipated role for cohesin and further suggest a widespread role for the selective formation of dsRNA, heterochromatin, and subsequent cohesin recruitment in regulated transcriptional termination.

INTRODUCTION

The compressed nature of yeast genomes (*S. cerevisiae* and *S. pombe*) places severe constraints on the ordered processes of gene transcription, DNA replication, and mitosis. Thus, yeast protein encoding genes are closely spaced and possess few introns, and their transcription units have tightly defined borders (Bahler, 2005). Transcription initiation generally occurs at unique start sites and terminates soon after the polyA (pA) signal at the end of the gene's 3′UTR. In contrast, for highly intronic mammalian genes there are often multiple or ill-defined transcription start sites and termination may occur several kilobases beyond the pA signal. Significantly, gene defects in the myriad of factors required to define the ends of transcription units are often lethal to yeast (Zhao et al., 1999). Inactivation of 3′-end formation causes readthrough transcription that may result in transcriptional interference of downstream genes when arranged in tandem (Shearwin et al., 2005). This inhibitory process is thought to occur by blocking access of transcription initiation factors to the promoter of the downstream gene, so that RNA polymerase II (Pol II) is prevented from initiating transcription (Greger et al., 2000). For genes arranged in convergent orientation, failure of Pol II to terminate transcription may also result in inhibition of gene expression due to collision of elongating Pol II complexes (Prescott and Proudfoot, 2002). Both transcriptional interference and collision have been shown to regulate *S. cerevisiae* gene expression in specific cases (Hongay et al., 2006 and Martin et al., 2004).

Transcriptional termination is also paramount for the correct regulation of replication origin, telomere, and centromere function. Transcription readthrough into any of these chromosomal elements due to defective termination results in the loss of genome integrity during replication and mitosis (Chen et al., 1996; Hegemann and Fleig, 1993). However, a specific situation where interplay between transcription and mitosis occurs relates to the protein cohesin. This multisubunit protein complex plays essential roles in sister chromatid cohesion and faithful chromatid segregation into daughter cells. In *S. cerevisiae* it contains two SMC subunits, Smc1 and Smc3, which dimerize to form a V-shaped molecule. The other tips of their arms contain ABC-like ATPase domains that are connected by an α kleisin subunit, called Scc1 or Rad21 in *S. pombe* (Hirano, 2006; Nasmyth and Haering, 2005; Nonaka et al., 2002; Tanaka et al., 1999). Cohesin forms a large protein ring encircling the DNA strands (Haering et al., 2002) and is loaded onto chromosomes at multiple positions in early G2 in part by Ssc2/Ssc4 loading protein complex (Ciosk et al., 2000). High levels of cohesin are known to localize to heterochromatic regions of chromosomes, especially on centromeres and telomeres and at the silent mating type loci. Here it is thought that the defining heterochromatic protein Swi6 (HP1 in higher eukaryotes) acts to recruit cohesin through direct interaction with both loading complex and cohesin Psc3 (Scc3 in *S. cerevisae*; Nonaka et al., 2002). An indirect involvement of transcription in *S. pombe* cohesin recruitment is evident since heterochromatin is itself formed in response of overlapping transcription profiles that induce the RNAi pathway. Nuclear Dicer activity converts this dsRNA into siRNA that as part of the RITS complex induces localized heterochromatin formation (Verdel and Moazed, 2005). This dsRNA is known to be synthesized by

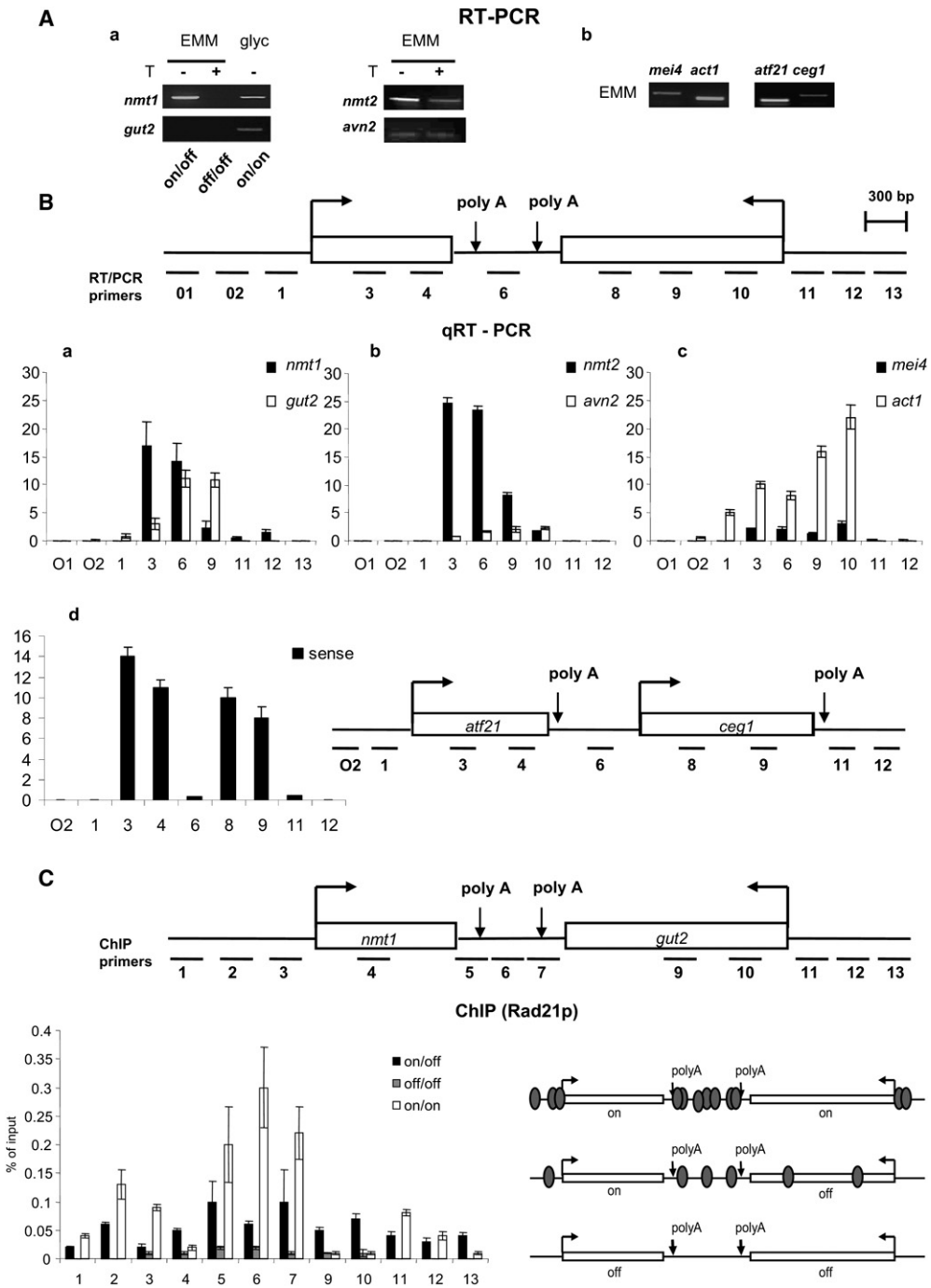

Figure 1. Overlapping Transcription and Cohesin Localization in Convergent Genes

(A) Expression patterns of all tested genes in EMM or glycerol media with or without thiamine were analyzed by RT-PCR using oligo dT and PCR using primers within each ORF.

(B) Diagram of primers used in RT-PCR (horizontal lines with numbers) for three convergent gene loci. Cells were grown in conditions where both genes are transcribed (glyc for *nmt1-gut2*, EMM for *nmt2-avn2*, and *mei4-act1*). mRNA levels were determined by quantitative RT-PCR using specific primer pairs and are shown graphically (a, *nmt1-gut2*; b, *nmt2-avn2*; c, *mei4-act1*). Primer efficiency was normalized using genomic DNA. Data shown represent average of at least three independent biological experiments. Minus RT controls validate data specificity (data not shown). d, RT-PCR analysis of tandem gene pair *aft21-ceg1*. Diagram shows positions of RT and PCR primers. Graph shows levels of mRNAs transcribed from sense strand. Antisense mRNAs were not detected. Y axis values show level of RT-PCR signal above background. Error bars represent ± standard deviation (SD) for each primer pair performed in triplicates. (C) See next page.

Pol II in *S. pombe* although in plants a dedicated Pol IV enzyme is involved (Herr et al., 2005). The extent and promoter specificities of these heterochromatin transcripts are unknown. Furthermore the low levels of these transcripts are amplified by RNA-dependent RNA polymerase (Rdr) activity (Motamedi et al., 2004).

Lower levels of cohesin also associate throughout chromosomes, outside heterochromatin centers. For this cohesin population it is thought that active transcription realigns cohesin leading to its accumulation between convergent transcription units. Possibly the passage of elongating Pol II somehow acts to concentrate cohesin into this specific location. In particular, inactivation of one gene from a convergent gene pair results in the failure of cohesin to properly localize prior to mitosis (Glynn et al., 2004; Lengronne et al., 2004). We describe experiments in *S. pombe* that lead to an understanding of how intergenic cohesin is repositioned during the cell cycle. These studies were prompted by earlier work from this lab indicating that for two genes *nmt1* and *nmt2*, their nascent transcripts extend into downstream convergent genes (Hansen et al., 1998). We began these studies by confirming that convergent genes generate significant levels of overlapping transcript. Furthermore by synchronizing *S. pombe* in the G1 or G2 phase of the cell cycle we show that these overlapping dsRNA transcripts are G1 specific since in G2, intergenic cohesin acts to promote gene-proximal transcription termination, so preventing the continued synthesis of dsRNA. Following on from these results we show that G1-specific dsRNA from these convergent genes induces localized transient heterochromatin formation (histone H3 lysine 9 trimethylation [H3K9me3] and Swi6 recruitment) through the combined action of Dicer and RITS. Consequently inactivation of Dicer (Dcr1) or the argonaute subunit (Ago1) of RITS causes loss of G1-specific heterochromatin over convergent genes as well as continued dsRNA synthesis in G2. Furthermore inactivation of Swi6 causes loss of cohesin recruitment. These results suggest a cycle of G1-specific dsRNA and heterochromatin formation followed by G2 cohesin recruitment and gene-proximal termination.

RESULTS

Convergent genes in *S. pombe* account for less than 20% of Pol II-transcribed genes. They also possess unique structural features with unusually short intergenic regions of about 600 bp and multiple pA signals (Sanger Institute). Transcription run on analysis (TRO) of Pol II-transcribed genes in *S. pombe* to define the extent of their transcription unit has only been carried out in a few specific cases. For example we have previously characterized the *ura4* transcription unit by TRO showing that termination occurs shortly following the gene-proximal polyA signal (Birse et al., 1997). *Ura4* is located in tandem orientation with respect to its adjacent genes. In contrast, our subsequent studies on the highly expressed *nmt1* and *nmt2* genes showed that TRO-detected nascent transcription extends beyond their pA sites and overlaps with convergent *gut2* and *avn2* genes, respectively (Hansen et al., 1998).

Convergent Genes of *S. pombe* Display Overlapping Transcription Patterns

We wished to determine if readthrough transcription was a general feature of convergent gene pairs. We therefore focused our analysis on four different gene pairs, three convergent loci (*nmt1-gut2, nmt2-avn2*, and *mei4-act1*), and one control tandem gene pair (*atf21-ceg1*), initially determining their mRNA expression levels by RT-PCR using oligodT and specific primers for each ORF (Figure 1A). For *nmt1-gut2* it was possible to differentially regulate transcription by varying growth conditions, allowing both genes to be active (on/on) or inactive (off/off) or to have only *nmt1* active (on/off). Thus *nmt1* is expressed in both EMM and glycerol medium and is repressed by thiamine in EMM, while *gut2* is expressed only in glycerol medium. Both *nmt2* and *avn2* genes are transcribed in EMM medium with or without thiamine, although thiamine does significantly reduce *nmt2* expression (Figure 1Aa). The other convergent gene, pair *mei4-act1*, is expressed in EMM medium and unaffected by thiamine as is the tandem gene pair *atf21-ceg1* (Figure 1Ab).

We next performed quantitative transcription analysis on these four gene loci to determine the extent of transcription across each convergent gene loci (Figure 1B). *S. pombe* was grown under conditions where all tested genes are expressed. Total RNA was analyzed by RT-PCR using specific RT primers for both strands followed by the same primer plus an upstream primer to amplify specific transcript regions. Products were analyzed and quantified by real-time PCR. Primer pair efficiency was normalized using genomic DNA as template. To analyze transcription of the *nmt1-gut2* locus, cells were grown in glycerol medium. As expected, high signals were evident over the structural genes detected with primers 3, 6, and 9 for both forward and reverse RT primers. The furthest 3′ signal above background for *nmt1* was with primer 12 and for *gut2* primer 1 (Figure 1Ba). Consequently, these data suggest that readthrough transcription occurs from both genes on both strands. In effect the *nmt1* promoter appears to double as a terminator region for *gut2* while the *gut2* promoter overlaps with the terminator region of *nmt1*. RT/PCR analysis of *nmt2-avn2* and *mei4-act1* loci gave similar results (Figures 1Bb and 1Bc). Note that *nmt1* and *gut2* transcript levels are near equal while *nmt2* and *act1* transcripts are at much higher levels than those of their convergent gene partners as shown above (Figure 1A). We also investigated the potential readthrough in the tandem oriented genes *atf21-ceg1* (Figure 1Bd). RT-PCR analysis shows high signals with probes 3, 4, 8, and 9, which are in ORFs of either gene. However, we did not detect significant signal with the intergenic primer 6. We also performed RT-PCR analysis to detect possible transcripts from the *atf21-ceg1* antisense DNA strand, but no positive signal was obtained (data not shown).

The above transcription analysis of three convergent cotranscribed gene pairs (but not the tandem control gene pair) indicates that a surprising level of readthrough transcription occurs for each gene. These data are particularly unexpected in view of the well-documented presence of cohesin complex

(C) Cohesin ChIP analysis for *nmt1-gut2* locus. Positions of PCR primers (horizontal lines with numbers) are indicated. *rad21-GFP* cells were grown in glyc (on/on) or EMM with (off/off) or without T (on/off). Fragmented chromatin was immunoprecipitated with anti-GFP antibody and analyzed by quantitative PCR. Error bars as in (B). Diagram summarizes localization of cohesin based on ChIP analysis. Actively transcribed genes are indicated.

concentrated between convergent genes particularly in the G2 cell-cycle phase (Lengronne et al., 2004). To confirm that cohesin is indeed present between the convergent genes analyzed in this study, we next performed ChIP analysis on chromatin isolated from a GFP-tagged cohesin (*rad21)* strain grown in glycerol (on/on), EMM (on/off), and EMM+thiamine (off/off) medium using anti-GFP antibody (Figure 1C). Our results show that Rad21 concentrates in the *nmt1-gut2* intergenic region under on/on conditions. Intergenic localization of Rad21 was reduced, when only *nmt1* gene was expressed (on/off). Here all primers show signals of similar intensity. Even primers 10–13, which are positioned beyond the promoter of *gut2*, gave significant signal, suggesting that cohesin slips away, "pushed" by the elongating Pol II complex transcribing *nmt1*. No significant cohesin localization was observed when transcription of both genes was switched off. We also note that significant Rad21 ChIP signal was detected with primers 2, 3 and 11, 12 in on/on conditions. These cohesin signals in the promoter region may reflect gene looping between either end of each convergent gene (unpublished data). We also performed ChIP analysis on the *mei4-act1* gene pair as previously described (Lengronne et al., 2004). As with *nmt1-gut2* in the on/on condition we observed an intergenic accumulation of Rad21 (Figure S1B available online). To confirm that cohesin localization is enriched in G2, we performed ChIP analysis on *nmt2-avn2* using *cdc10* and *cdc25* mutant strains to arrest cell cycle in G1 or G2, respectively. For these experiments we employed a polyclonal anti-rad21 antibody (Figure S1C). Positive signals in the intergenic region as well as over the promoter region caused by gene looping were obtained with G2 chromatin while lower signals were observed for G1 chromatin. We finally wished to establish that the cohesin loading complex was also associated with these convergent genes. We detected a significant ChIP signal over the promoter regions of the *nmt2-avn2* and *mei4-act1* loci with GFP antibody on chromatin from a strain bearing a *mis4* GFP genomic tag (Figure S1D). Mis4 is the *S. pombe* homolog of the Ssc4 subunit of the *S. cerevisiae* loading complex (Bernard et al., 2008). We synchronized cell populations in G1 or G2 using hydroxyurea treatment (Experimental Procedures) and detected Mis4 in both cell-cycle phases, though somewhat more in G1. These data suggest that cohesin loading complex recruits cohesin to the promoter regions of these convergent genes. This recruited cohesin is then repositioned to the intergenic region by Pol II elongation in G2 (Lengronne et al., 2004).

Overall our ChIP analysis on cohesin placement in the three convergent gene loci used here supports previous studies (Lengronne et al., 2004) and consequently raises the interesting paradox of how these genes can generate readthrough transcription in the presence of cohesin complex, which is likely to impede such transcription.

Transcriptional Termination and mRNA 3′-End Formation at the Major pA Site in G2

The above results (Figure 1) suggest that the tested convergent genes generate readthrough transcripts, even though when cohesin is present in their intergenic regions in G2, a block to such transcripts is predicted. We therefore tested if the readthrough transcription profiles we observe are themselves cell cycle specific. We employed *cdc10* and *cdc25* mutants to block *S. pombe* in either G1 or G2. Cells were grown in EMM medium at permissive temperature and then blocked by shifting to restrictive temperature. The DNA content of the cells was determined by FACS analysis (Experimental Procedures) and total RNA from either G1 or G2 cells was isolated and subjected to quantitative RT-PCR (Figure 2A). Additional primers were employed to focus more closely on the intergenic region. RT/PCR analysis was applied to both the *nmt1-gut2* and *nmt2-avn2* genes with cells grown in EMM medium. Consequently *nmt1-gut2* was in the on/off transcription state while both *nmt2* and *avn2* were transcriptionally active. This growth condition allowed us to compare bidirectional versus unidirectional transcription in G1 and G2.

As with unsynchronized *S. pombe* (Figure 1A), we observed significant RT-PCR signals in G1 on both strands with all primers 2–10, corresponding to a bidirectional readthrough profile across the *nmt2-avn2* locus. Note that *nmt2* mRNA levels were 10-fold higher than *avn2* as seen above (Figure 1A). This readthrough profile was abolished in G2 so that for *nmt2* the last positive signal was detected with primer 6, just after the proximal *nmt2* pA site (Figure 2Aa). Similarly for *avn2,* primer 7 gave the last positive signal in G2, which covers the *avn2* major pA site (Figure 2Ab). In contrast, the readthrough transcription profile of *nmt1* did not change significantly between G1 and G2 (Figure 2Ac). These data strongly suggest that transcriptional readthrough is G1 specific and is lost in G2, but only if both convergent genes are transcribed.

We wished to confirm the above RT/PCR data by mapping pA site usage for both *nmt1* and *nmt2* grown in EMM medium (on/off and on/on, respectively). We therefore performed 3′RACE analysis using phased oligodT RT-PCR analysis (Figure 2B) with total RNA from cells blocked in G1 or G2. cDNA obtained was PCR amplified using nested primers within the *nmt1* or *nmt2* ORFs and fractionated on agarose gels. We observed two major bands for the *nmt1* gene (Figure 2Ba) in both G1 and G2. These correspond to mRNA using either proximal or downstream cryptic pA sites (Figure 2Ba). This mRNA profile reflects the high levels of readthrough transcripts as seen above. 3′RACE of *nmt2* again confirms the RT/PCR patterns (Figure 2Bb). Multiple bands are visible in G1, all corresponding to mRNAs employing cryptic pA signals beyond the proximal pA site. Remarkably, this pattern changes in G2. Here we observed only one strong band corresponding to *nmt2* mRNA ending at the proximal pA site (Figure 2Bb). Consequently, these results are in agreement with quantitative RT-PCR analysis (Figure 2A). The cryptic pA sites, used for *nmt1* or *nmt2* mRNA in G1, lie in regions corresponding to pA sites of the convergent downstream gene. The possibility that these pA sites function in both directions will require further investigation.

We finally performed transcription run on (TRO) analysis on *nmt1* and *nmt2* genes using G1 and G2 cells. In outline, *cdc10* or *cdc25* mutants were grown in EMM medium, blocked in G1 or G2 by temperature shift, and subjected to TRO analysis using M13 single-strand DNA probes (Hansen et al., 1998). Analysis of *nmt1* showed positive signals across the ORF (probe 1), intergenic region (probes 2, 3, and 4), and downstream convergent *gut2* gene (probe 5). However, note that we did observe a 50% reduction in TRO signal beyond the *nmt1* polyA signal. The

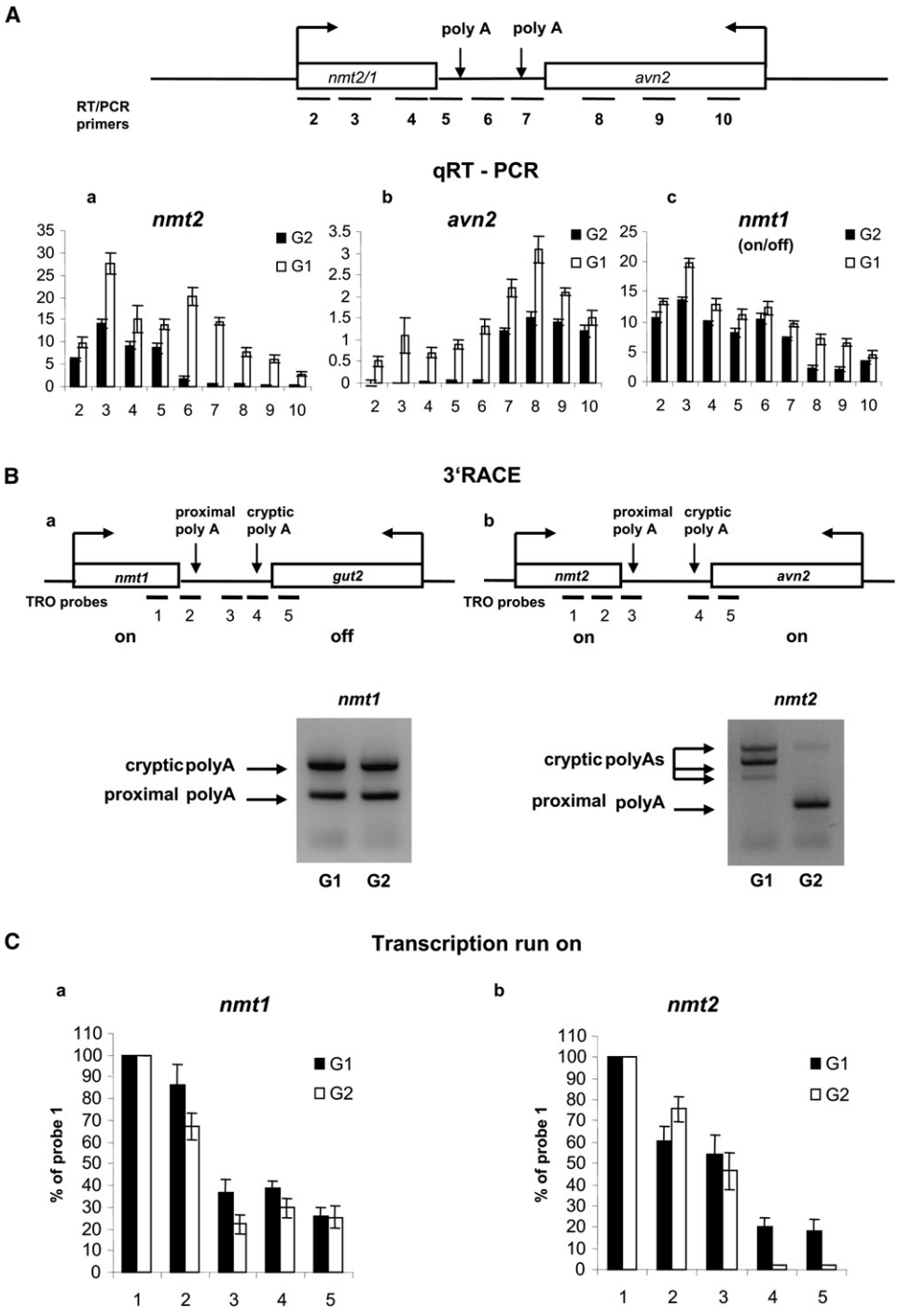

Figure 2. Gene-Proximal pA Site of Convergent Genes Is Selected in G2

(A) Diagram of primers used for RT-PCR analysis of *nmt1-gut2* and *nmt2-avn2* transcription. Temperature-sensitive mutants *cdc10* and *cdc25* were grown in EMM medium and blocked in G1 or G2. Total RNA was isolated and steady-state levels of mRNA were determined by quantitative real-time RT-PCR as in Figure 1B. Error bars represent ± SD from triplicate experiments. Graphs (a–c) show mRNA levels for specified gene. Black bars represent mRNA levels in G2 phase, white bars represent mRNA levels in G1 phase.

(B) G1- or G2-specific mRNAs (as in A) were analyzed by 3′RACE: *nmt1* gene (a), *nmt2* gene (b). Transcripts using proximal or cryptic pA sites are indicated.

(C) Transcription run on analysis of synchronized cells. *nmt1* gene (a), *nmt2* gene (b). Positions of M13 single-stranded probes are shown in 2B (horizontal lines with numbers). Black bars in graphs correspond to G1 and white bars G2 cells. TRO signals were normalized to probe 1 and expressed as % of probe 1. Values in graphs were determined as averages of three independent biological experiments (± SD) (Figure S2).

profiles obtained were very similar in G1 and G2 (Figures 2Ca and S2), indicating that significant levels of nascent transcription read through *nmt1* throughout the cell cycle. In contrast, analysis of the *nmt2* gene showed significant signals with all probes in G1 with again a 50% reduction in TRO signal following the *nmt2* pA signal (compare probes 3 and 4), but in G2 the profile has changed. The last positive signal above background was detected with probe 3 corresponding to the *nmt2* proximal pA site (Figures 2Cb and S2). These results demonstrate that in G2, transcription termination occurs immediately following the proximal pA site.

Based on our combined RT/PCR, 3′RACE, and TRO results, we conclude that the transcription readthrough profile is specific for G1 but remains unchanged for unidirectional transcription units in G2. However, in situations of convergent transcription both steady-state and nascent transcripts terminate immediately following the gene ORF in G2 but readthrough into the convergent gene in G1.

Cohesin Complex Promotes mRNA 3′-End Formation and Transcriptional Termination

The observed transcription dependence and G2 specificity of 3′-end formation for convergent gene transcripts (Figures 1 and 2) matches the localization properties of cohesin (Figures 1C and S1; Lengronne et al., 2004). This strongly suggests a connection between cohesin and 3′-end formation events. We therefore sought to establish a direct influence of cohesin on 3′-end formation and transcription termination. Wild-type (WT) and ts mutant *rad21-K1* cells (Tomonaga et al., 2000) were grown overnight in EMM-T medium lacking nitrogen source to block them in G1. Cells were than shifted to nitrogen-rich medium at 37°C for 6 hr to reach G2 and also to inactivate Rad21 in the *rad21-K1* ts mutant strain (Experimental Procedures). DNA content was then determined by FACScan showing that the cell populations were largely restricted to either G1 (1N) or G2 (2N) cell-cycle phases (Figure 3A). Rad21 protein levels were also measured by western blot analysis using anti-Rad21 antibody (Figure S3). As indicated the *rad21-K1* cells showed a significant loss of Rad21 in G2 samples following temperature shift to 37°C.

Total RNA was isolated from blocked WT or *rad21-K1* cells and used as a template for 3′RACE. PCR was performed with forward primers within *nmt1* or *nmt2* ORF. Under the EMM-T growth conditions employed, the *nmt1-gut2* locus was in the on/off state and *nmt2-avn2* was in the on/on state. While *nmt1* transcripts gave identical readthrough 3′RACE patterns in G1 and G2 in both strains, *nmt2* transcripts showed a switch from readthrough to mRNA using the proximal pA signal in WT, but critically not in *rad21-K1* cells. Consequently, these data establish that loss of the cohesin subunit Rad21 causes a coincident loss of *nmt2*-proximal RNA 3′-end formation (Figure 3B). These results therefore predict that cohesin promotes gene-proximal polyadenylation by blocking readthrough transcription from the *nmt2* gene into the downstream convergent *avn2* gene. To validate the generality of this observation, we repeated 3′RACE analysis on three additional genes, *tea3, mei4*, and *pdt1*. These were selected because of their convergent arrangement with the downstream gene and because all of these convergent genes are expressed in EMM growth conditions (Figure 1Ab and data not shown). We observed significant changes in all tested genes, from readthrough profile in WT G1 cells to a single mRNA using its proximal pA signal in WT G2 cells. However, this observed pA site switch is lost if the level of Rad21 is decreased to a minimum (Figure 3B). It is notable that the levels of mRNA using the proximal pA site in G1 varied from gene to gene. We predict that *tea3* has a weak proximal pA site, *mei4* and *nmt2* have moderate proximal pA sites, and *pdt1* possesses a strong proximal pA site. Even so it is striking that for each convergent gene pair a switch from readthrough to near complete proximal pA site usage is induced by the cohesin protein complex.

To establish that cohesin directly influences transcription termination, we also performed transcription run on analysis on the *nmt2-avn2* gene pair. WT and *rad21-K1* cells were blocked in G1 phase by nitrogen starvation. The block was then released by further incubation in EMM+N medium at 37°C. This allowed cells to proceed into G2 phase and also to decrease levels of Rad21 in *rad21-K1* cells to a minimum. Transcription run on data showed that Pol II reads through in WT G1 cells. This profile is lost in WT G2 cells, where TRO signal for probe 4 is significantly reduced, reflecting Pol II termination after the proximal pA signal. In contrast, readthrough profile was observed in *rad21-K1* cells for both G1 and G2 (Figure 3C). These results imply that G2-specific cohesin promotes transcriptional termination.

Convergent Cotranscribed Genes Display G1-Specific Transient Heterochromatin

The G1-specific readthrough transcription profile observed for convergent gene loci as investigated in this study raises the intriguing possibility that in G1 these loci will generate long stretches of dsRNA. However it is also possible that although we detect overlapping transcripts in the whole cell population, individual cells may express only one strand of each readthrough transcript. If localized dsRNA does exist in G1 then we might expect it to induce the RNAi gene silencing pathway, as demonstrated for the heterochromatic centromeres of *S. pombe* (Volpe et al., 2002). Furthermore if the observed G1-specific overlapping transcription profiles are truly general for all convergent genes, this would suggest that a large number of such genes are silenced and heterochromatic in G1.

We carried out ChIP analysis on G1- and G2-specific chromatin samples using HU treatment to synchronize cells to either G1 or G2 (Experimental Procedures) for *nmt1-gut2*, *mei4-act1*, and *nmt2-avn2* in on/off and on/on transcription conditions, respectively. Fragmented chromatin was immunoprecipitated with heterochromatin-specific antibodies for H3K9me3 and Swi6-GFP epitopes. *nmt1-gut2* was in an on/off state and so cannot generate dsRNA. Therefore no positive ChIP signals were detected with either heterochomatin-specific antibody (Figures 4A and 4B). Note that significant signals were detected with both G1 and G2 chromatin for the positive control centromeric ChIP primers. Also a positive ChIP signal was detected using a polyclonal H3 antibody and primer 3 for each gene pair. In marked contrast to *nmt1-gut2* on/off chromatin, *nmt2-avn2* on/on chromatin gave strong G1- but not G2-specific heterochromatin signals across the whole locus (Figures 4C and 4D) but was reduced to background levels upstream of each promoter. These data demonstrate the existence of a transient heterochromatin

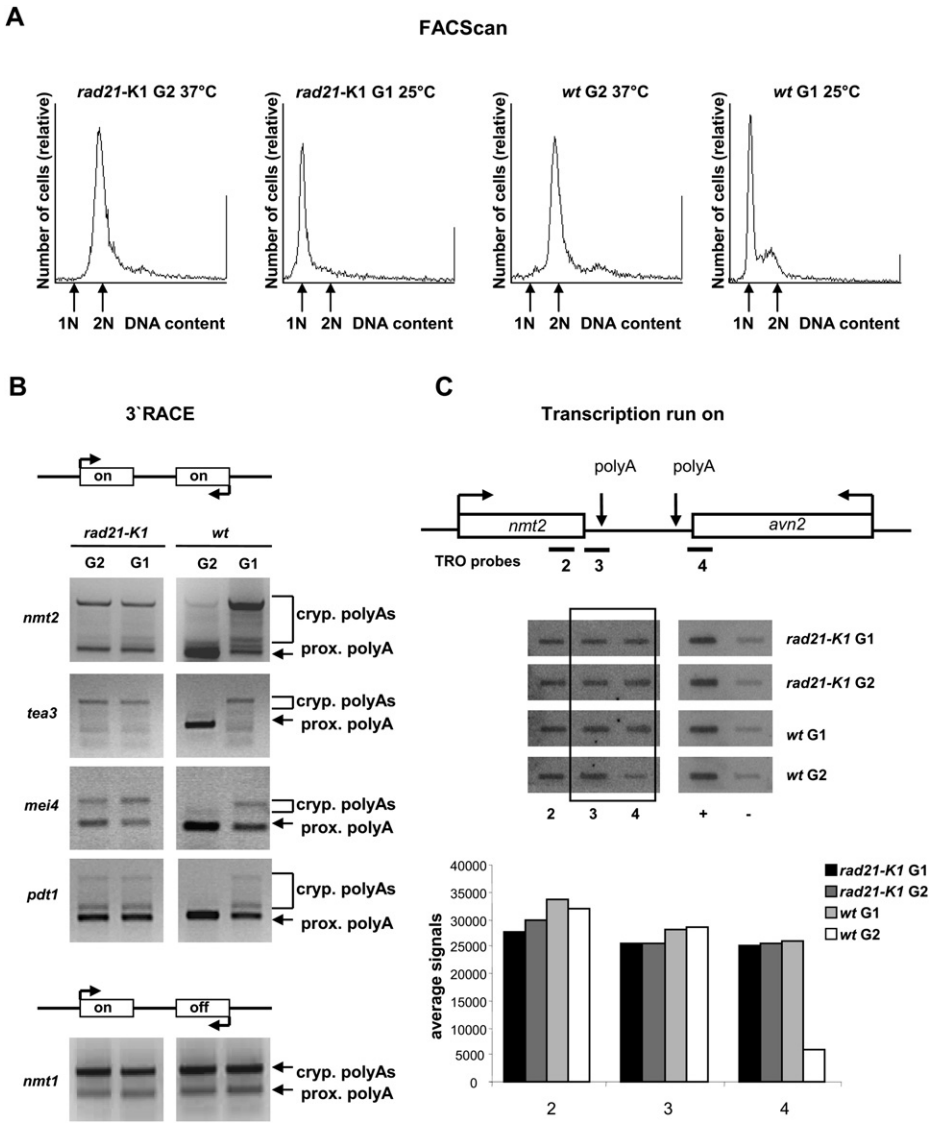

Figure 3. Cohesin Complex Promotes Proximal pA Site Selection

(A) WT and *rad21-K1* cells were blocked in G1 phase by nitrogen starvation. Block was released by changing the medium to EMM with nitrogen source. Cells were also shifted to 37°C and incubated for 6 hr. DNA content was measured by FACScan analysis, as shown. Positions of 1N and 2N DNA are indicated (see Experimental Procedures).

(B) Total RNA was analyzed by 3′RACE. Transcripts using the proximal or cryptic pA sites are indicated. Analysis of four tested genes in on/on conditions is shown. Lower panels show results of *nmt1* 3′RACE in on/off condition. WT or *rad21-K1* cells are indicated above the panels, as well as G2 and G1 phases.

(C) Transcription run on analysis of *nmt2-avn2*. WT and *rad21-K1* cells were grown in EMM medium and synchronized by nitrogen starvation. Experiment repeated twice and graph shows average values. Box denotes switch in termination profile.

domain across this locus. Furthermore the cotranscribed convergent *mei4-act1* locus also displays G1-specific heterochromatin marks in an analogous fashion to *nmt2-avn2* (Figures 4E and 4F). These significant data suggest that a widespread class of G1-specific heterochromatin exists in the *S. pombe* genome and is associated with transcribed, convergent genes.

The presence of heterochromatin marks and in particular Swi6 across transcribed convergent gene loci provides an immediate explanation for how cohesin can be specifically recruited to these genomic loci. Thus the cohesin ring subunit Psc3 is known to interact with Swi6 in heterochromatic regions such as the centromere, and this specific interaction is considered to be a key feature of the recruitment process of cohesin to heterochromatin (Nonaka et al., 2002). We therefore employed an *S. pombe* strain deleted for *swi6* and possessing a GFP-tagged cohesin subunit gene, *psc53*. In the isogenic WT strain (also containing *psc53-GFP*), ChIP analysis was performed with anti-GFP antibody across the cotranscribed convergent gene loci, *nmt2-avn2 and mei4-act1* (Figures 5A and 5C). As for Rad21 localization (Figures 1C and S1), both loci gave strong positive cohesin signals in the

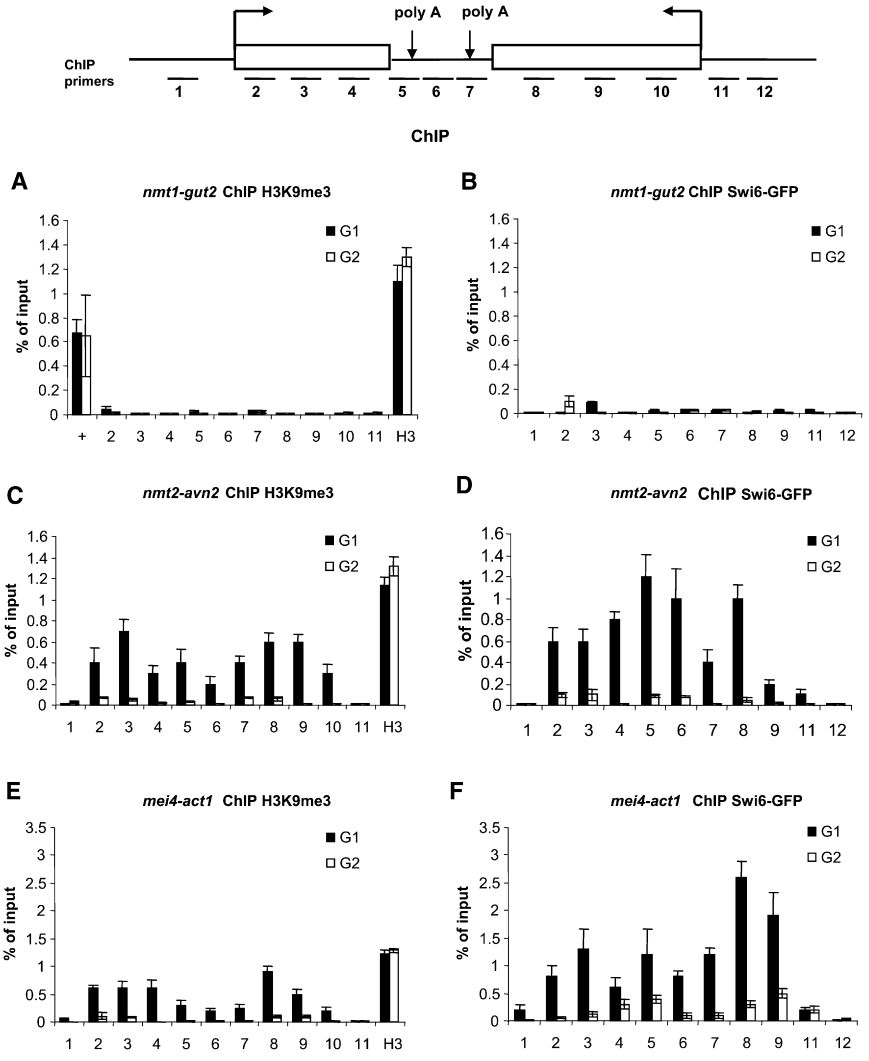

Figure 4. Transient Heterochromatin Is Formed between Convergent Genes in G1

Diagram shows positions of PCR primers and proximal polyA sites. Cells were grown in EMM medium and synchronized to either G1 or G2 by HU treatment. ChIP experiment was performed using either anti-H3K9 trimethylated or GFP antibodies. Latter antibody was used to detect Swi6 from cells expressing GFP-tagged Swi6. *nmt1-gut2* (A and B), *nmt2-avn2* (C and D), *mei4-act1* (E and F) ChIP analysis for either H3K9trime or Swi6 detection. In addition, ChIP with anti-H3 antibody was performed as positive control for primer 3 in each gene pair (A–F). Also in graph A, + represents primer to detect centromeric sequence. Histograms show average values from three independent experiments. Error bars ± SD.

intergenic and promoter regions for G2 but less in G1-isolated chromatin. In the *swi6* deletion strain, the G2-specific signal was reduced to much lower levels (Figures 5B and 5D). Finally for the *nmt1-gut2* on/off locus only background signal was obtained for either G1- or G2-specific chromatin in either WT or *swi6* deletion strains (Figures 5E and 5F). It should be noted that all for six ChIP experiments (Figures 5A–5F) the same H3 antibody ChIP control, using primer 3 for each gene pair, was employed giving near equal G1 and G2 signals. This positive control allows crosscomparison within this data set.

Overall the data presented in Figures 4 and 5 provide compelling evidence that cotranscribed, convergent genes in *S. pombe* display a transient G1-specific heterochromatin mark, and furthermore this mark acts to recruit cohesin complex to these chromosomal regions in G2.

G1-Specific Heterochromatin and Readthrough Transcription in Convergent Genes Are Associated with RNAi

We finally investigated the role of the RNAi pathway in convergent gene heterochromatin and transcriptional regulation. In particular we tested whether deletion of genes encoding either Dicer or the RITS component, Ago1, prevented G1-specific heterochromatin formation. We also determined whether loss of these activities as well as Swi6 resulted in continued overlapping readthrough transcription in G2 due to the lack of RNAi-mediated dsRNA degradation and consequent lack of cohesin recruitment.

ChIP analysis (Figure 6A) was performed to detect H3K9me3 and Swi6 in G1 as before (Figure 4) using primers specific for either the *nmt2-avn2* or *mei4-act1* loci, but with *ago1* and *dcr1* deletion strains, as compared to WT. For both deletion strains with each primer pair tested, we observed a significant reduction in ChIP signals to 10%–20% the levels of WT. A similar loss in heterochromatin marks was observed using the centromeric primers. These data confirm that the G1-specific heterochromatin mark is indeed dependent on the RITS complex and Dicer as for centromeric heterochromatin.

We next performed 3′RACE analysis on the convergent gene set used before (Figure 3B). We again employed RNA samples isolated from G1- and G2-phased (by HU treatment) WT, *Δago1, Δdcr1*, or *Δswi6* cells. Similarly to loss of cohesin, we show that knockout of any one of these RNAi pathway-associated factors as compared to WT causes a complete loss of G2-specific proximal polyA site selection. Thus WT G1 and G2 RNAs gave clear shifts from readthrough transcription causing cryptic pA site usage to exclusive use of the proximal pA site (Figure 6B). In dramatic contrast each of the deletion strains gave a readthrough pA site usage profile in both G1 and G2 RNA samples. Again the *nmt1-gut2* on/off locus provides a clear control showing that these RNAi components only act on convergent gene loci that are capable of generating dsRNA. In this case, use of the distal cryptic polyA site dominated in both G1 and G2 for all the strains.

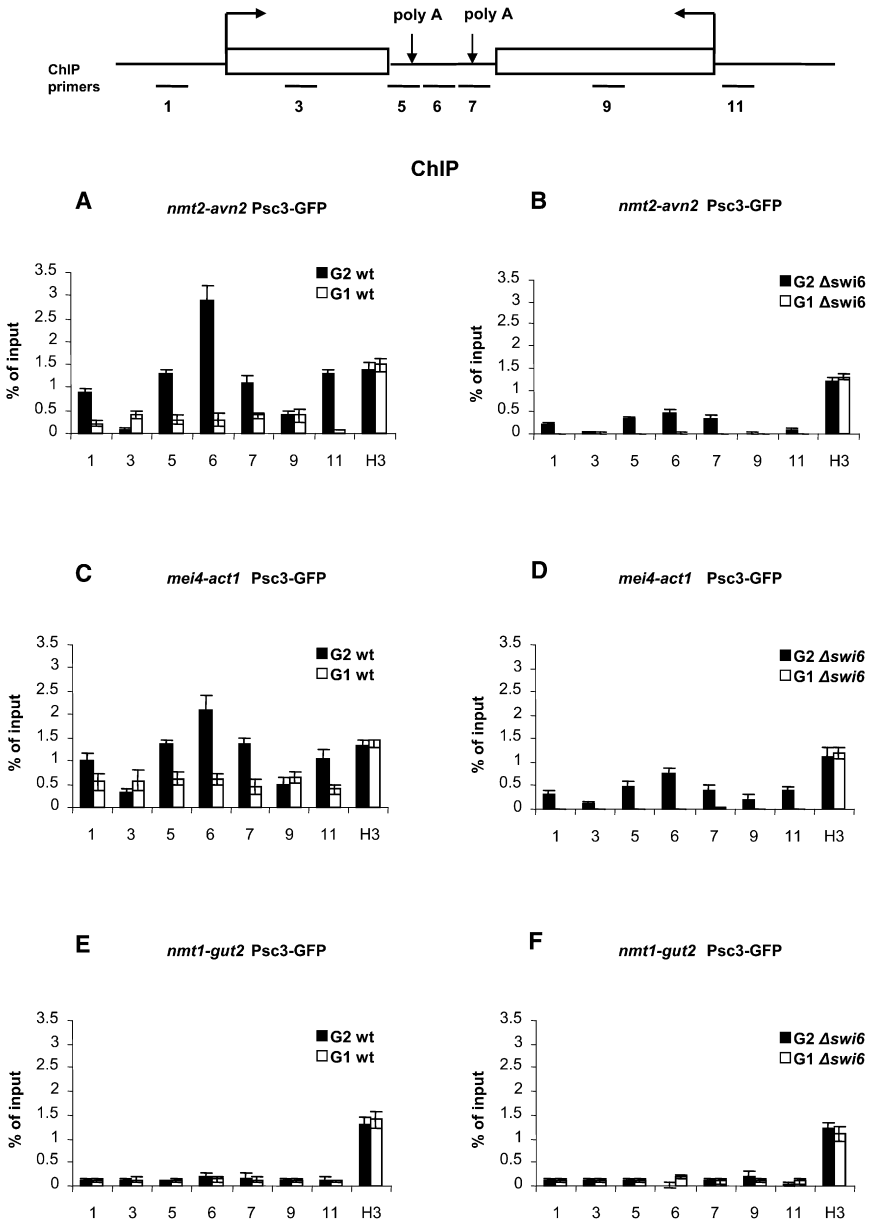

Figure 5. Cohesin Localization Is impaired by Lack of Swi6 between Convergent Genes

Positions of ChIP primers and proximal polyA sites are summarized in diagram. Cells expressing Psc3-GFP were grown in EMM medium and synchronized by HU treatment. ChIP analysis of *nmt2-avn2* gene pair (on/on) is shown. Signals in G1 or G2 in WT cells (A) correspond to positions of Rad21 in *cdc10* and *cdc25* ts mutants (Figure S1B). Signals of Psc3-GFP in cells lacking Swi6 are significantly reduced (B). Similar ChIP data were obtained for *mei4-act1* (on/on) gene pair (C and D). ChIP analysis of *nmt1-gut2* (on/off) reveals no significant Psc3 signals across gene pair (E and F). In parallel, ChIP analysis was performed with anti-H3 antibody with primer 3 as positive control (see signal H3 in each graph). Histograms show average values from three independent experiments. Error bars ± SD.

Finally these polyA site selection results were confirmed by TRO analysis on the *nmt2* gene in *Δdcr1*, *Δago1*, and *Δswi6* mutant cells as compared to WT *S. pombe* all synchronized by HU treatment to G2 (Figure 6C). It should be noted that TRO signals were quite low for these strains. Both the effect of synchronizing cells as well as the effect of RNAi mutation caused slow growth phenotypes, which resulted in low TRO signals. Even so it is evident that the normal G2-specific termination profile seen in WT cells (compare probes 3 and 4) is lost in these mutant strains, which display a readthrough transcription profile as observed by 3′RACE analysis (Figure 6B). These TRO results were confirmed by analysis of unsynchronized WT and *Δago1* cells (Figure S4), which again showed a clear shift to more readthrough transcription in mutant cells. Note that unsynchronized *S. pombe* cells are predominantly in G2, which is the longest cell-cycle phase.

Overall these results demonstrate that G1-specific dsRNA is acted upon by the RNAi pathway to induce heterochromatin, which in turn recruits cohesion through Swi6 interaction to these convergent gene intergenic loci. Once cohesin is positioned at this specific location in G2 then readthrough transcription will be blocked until mitosis occurs. The resultant loss of cohesin complex and the reestablishment of overlapping transcription profiles begin the new G1 phase of the next cell cycle. In effect cohesin autoregulates its own recruitment throughout the cell cycle.

DISCUSSION

Studies on the regulation of gene transcription in eukaryotes have traditionally focused on the initiation stage, with controlled recognition of specific promoters providing both temporal and developmental gene regulation. More recently transcription elongation has been appreciated to involve a complex interplay between cotranscriptional pre-mRNA processing and alterations in elongation efficiency across often extensive transcription units (Proudfoot et al., 2002). However, regulated transcriptional termination has not been previously detected. Consequently a view emerges that this final stage in the transcription cycle is effectively a constitutive process, solely occurring to facilitate the recycling of Pol II back to new rounds of transcription initiation. In contrast our new results in *S. pombe* provide a striking and apparently genome-wide process of regulated termination that is required for the fundamental process of mitosis through the ordered recruitment of cohesin complex. In particular we have uncovered an unanticipated mechanism of regulated transcription termination for cotranscribed, convergent genes in *S. pombe* that is closely associated with cell-cycle

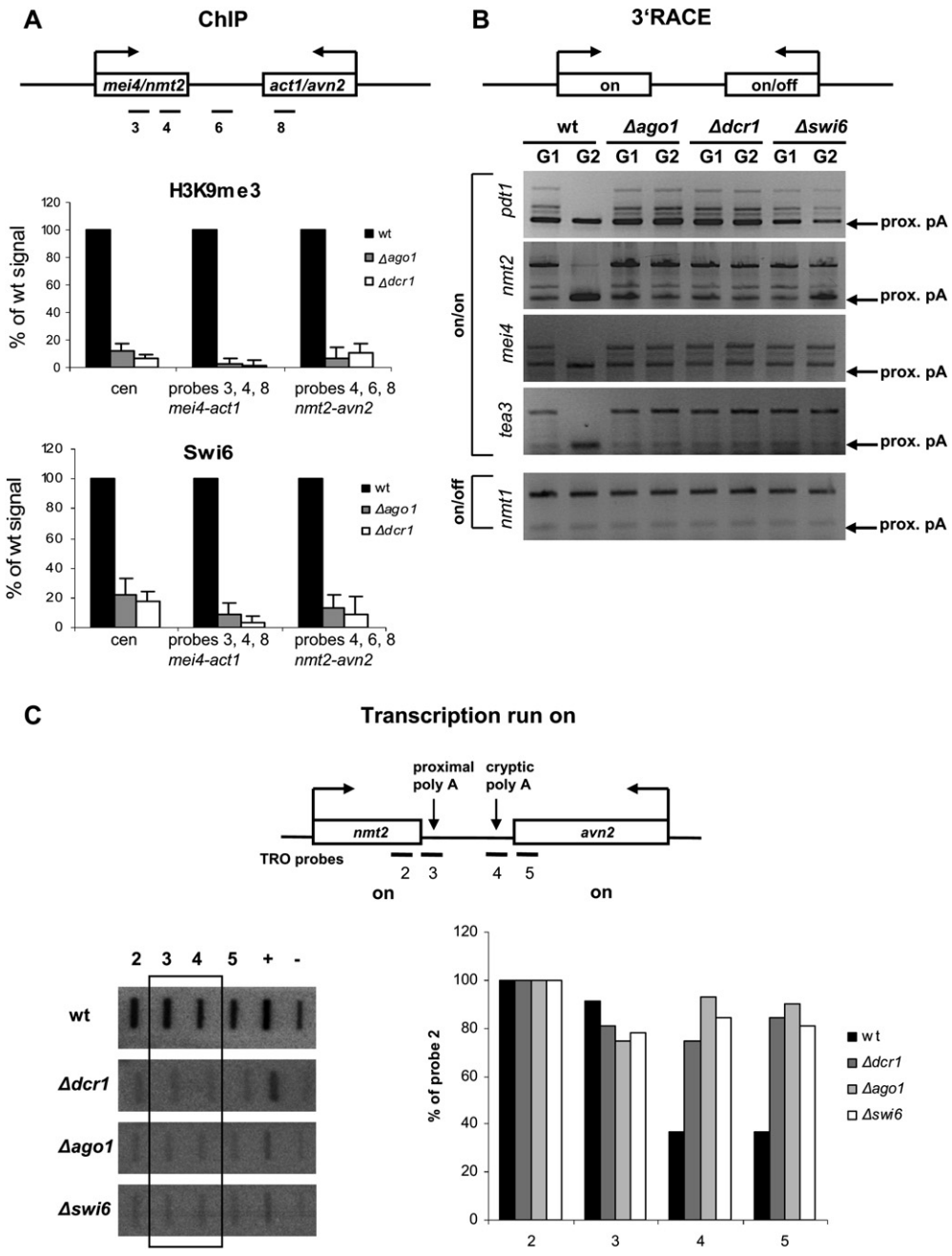

Figure 6. *ago1* and *dcr1* Deletion Impairs G1-Specific Heterochromatin and Promotes G2-Specific Readthrough Transcription in Convergent Genes

(A) ChIP analysis of selected probes across *nmt2-avn2* and *mei4-act1* gene pairs. WT, *Δago1*, and *Δdcr1* cells were blocked in G1 phase by HU treatment and immunoprecipitated using anti-H3K9me3 and anti-Swi6 antibodies. Average values of three probes for each gene pair were taken together and represented as a percentage of WT signal. Probe in centromere was used as control. Error bars ± SD.

(B) 3′RACE analysis of four convergent gene pairs in on/on conditions is shown. Proximal polyA site positions are indicated. Deletion mutants lacking *swi6, ago1*, or *dcr1* were grown in EMM medium and sychronized by HU treatment. Analysis of *nmt1-gut2* gene pair (on/off) is shown in bottom panel.

(C) TRO of G2 synchronized deletion mutant strains *swi6* and *ago1* versus WT on *nmt2-avn2* gene pair. Cells were grown in EMM medium, HU treated, and allowed to proceed into G2 phase. Diagram shows positions of probes and polyA signals. Signals were quantified by ImageQuant and are represented as percentage of probe 2 in graph. Box denotes switch in termination profile.

progression. These results raise a number of significant issues that we discuss in the context of the model for cell-cycle progression as shown in Figure 7.

Our results first reveal that in the G1 phase of the cell cycle, convergent genes generate high levels of readthrough transcription due to the apparent absence of transcriptional termination

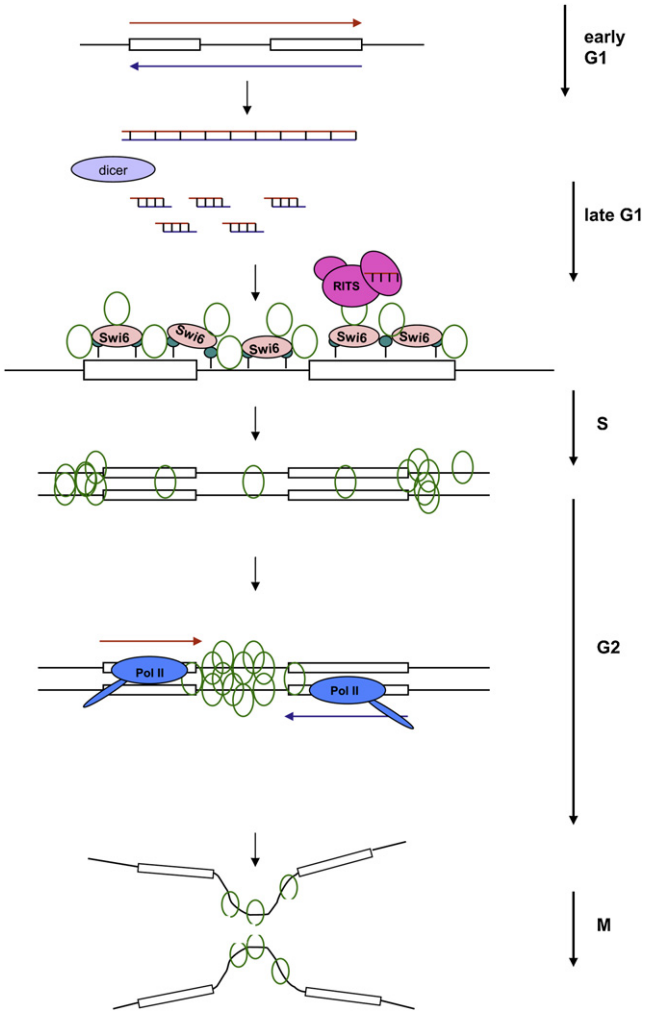

Figure 7. Model Showing Autoregulation of Cohesin Recruitment through dsRNA-Induced Heterochromatin Formation in G1 Leading to Transcription Termination in G2

Convergent gene pairs generate bidirectional readthrough transcripts in early G1. This leads to dsRNA formation, which is recognized and processed by Dicer into siRNA. RITS complex is activated and together with histone methyltransferase acts to methylate H3K9 (blue disc) over convergent gene loci. This is recognized by Swi6 (HP1 homolog) in late G1. Swi6 directly recruits cohesin (green rings) before and during early S phase. Swi6 may also help to recruit cohesin loading complexes (Ssl3, Mis4). During replication heterochromatin is removed allowing H3 to be acetylated and so promoting transcription. Because of cohesin's presence in G2, the Pol II complex is blocked in the intergenic region, promoting transcriptional termination after the proximal polyA site. The cohesin complex is relocalized and accumulates between convergent genes until M, when it is degraded during chromosomal separation. A new cell cycle recommences.

(Figure 2). These readthough transcripts are processed into polyadenylated mRNA at a range of cryptic polyA signals positioned apparently at random across the bicistronic loci. However, transcription does not extend beyond the downstream convergent promoter, possibly due to steric factors. It is striking that for the tandem genes tested, termination occurs closer to the proximal polyA signal (Figure 1Bd) possibly due to transcriptional pausing at this position. Such pausing effects have been previously described for the *ura4* gene (Aranda and Proudfoot, 1999). We predict that while tandem genes may possess pausing elements, these may be absent between cotranscribed convergent genes. Consequently the dsRNA generated by convergent gene readthrough transcription leads to the second phase in the cell-cycle model (Figure 7). Strikingly we show with two cotranscribed, convergent gene pairs (*nmt2-avn2* and *mei4-act1*) that a transient heterochromatin mark forms presumably in late G1. Importantly these heterochromatin marks are not apparent when only one of the two genes in a convergent gene locus is active (*nmt1-gut2*, on/off conditions). Thus we show that both H3K9 trimethylation and Swi6-containing heterochromatin are associated with *nmt2-avn2* and *mei4-act1* gene loci prior to the S phase (Figure 4). Furthermore Swi6 is required for subsequent cohesin recruitment, analogous to cohesin recruitment within centromeric heterochromatin (Figure 5). A key feature of the model presented in Figure 7 must be that dsRNA is fragmented by Dicer into RITS-associated siRNA. However, since these small RNAs are hard to detect for centromeric sequences we anticipate they will exist at even lower levels for these transient heterochromatin locations. We are currently devising sensitive detection strategies to search for these potential siRNAs. The next cell-cycle S phase apparently results in loss of the G1 heterochromatin mark but retains cohesin association, which is somehow carried through into G2. The loss of heterochromatin marks between G1 and G2 for the convergent genes studied here is particularly surprising. Such chromatin modifications are normally considered epigenetic, at least in permanent heterochromatin loci where they are maintained throughout mitosis. We predict that the heterochromatin observed in these studies is somehow afforded a more dynamic status, perhaps by the action of specialized histone demethylases to remove H3K9 trimethylation. Future work will concentrate on this interesting potential difference between permanent and dynamic heterochromatin. Once G2 commences we no longer detect the heterochromatic marks observed across the convergent gene loci in G1. However, we now observe cohesin concentrated within the intergenic regions, consistent with previous reports (Glynn et al., 2004; Lengronne et al., 2004). In this situation we lose the readthrough transcription profiles characteristic of G1 and instead see exclusive use of gene-proximal polyA signals as well as gene-proximal transcription termination. Clearly in this situation cohesin is functioning to block the passage of Pol II elongation, forcing abrupt termination. The switch from G1 readthough transcription to G2 gene-proximal termination is brought about by the RNAi-dependent heterochromatin process we have uncovered. Thus strains deleted for *dcr1* and *ago1* both display continued readthough transcription into G2 (Figure 6). Furthermore because loss of Swi6 causes loss of cohesin recruitment (Figure 5) and loss of cohesin also causes G2 readthrough transcription (Figure 3), our data allow us to genetically define each stage in the presented cell-cycle model (Figure 7).

Two recent studies are consistant with our proposed model for cell-cycle-regulated cohesin recruitment to convergent genes. First cohesin is shown to associate with *S. pombe* chromosomes in G1, dependent on the cohesin loading complex (Bernard et al.,

2008). Second centromeric transcriptional activity appears to be most active in the G1-S phase (Chen et al., 2008). This result mirrors our observations that overlapping transcription in convergent genes and consequent heterochromatin formation occur at this same short time period of the *S. pombe* cell cycle. However we predict that the G1-specific transient heterochromatin marks we detect over convergent genes may be structurally distinct to heterochromatin present throughout the cell cycle in centromeric regions.

A critical issue for our model of transient heterochromatin formation and cohesin recruitment in *S. pombe* is how general this mechanism is to other eukaryotes. In particular for *S. cerevisiae*, cohesin is also known to focus within intergenic regions of convergent genes, suggesting a similar cohesin recruitment mechanism to that seen in *S. pombe* (Lengronne et al., 2004). However, since *S. cerevisiae* lacks the RNAi pathway and heterochromatin marks (H3K9 trimethylation and Swi6/Hp1) found in *S. pombe* as well as in higher eukaryotes, a significantly different mechanism of cohesin recruitment may occur. Recent studies in *S. cerevisiae* have, however, implicated the role of cryptic unstable transcripts (CUTs) in the silencing of genes that may well share close parallels with other eukaryotes (Camblong et al., 2007; Proudfoot and Gullerova, 2007). It is therefore possible that regulated transcription termination through cohesin recruitment to CUT-associated chromatin may also occur for this eukaryote. Further studies will need to be carried out to establish how general our results in *S. pombe* are for other eukaryotes. Also it remains to be established whether G1-specific dsRNA formation is a general feature of all cotranscribed convergent gene loci in *S. pombe*.

EXPERIMENTAL PROCEDURES

Yeast Strains

S. pombe 972 h$^-$ was used in this study as wild-type strain. *cdc25-22 h*$^-$ and *cdc10-C4 h*$^-$ temperature-sensitive mutants used for G1 and G2 block were kindly provided by C. Norbury. Strains *rad21-GFP::kan h90 leu1 ade6-M210* and *rad21-K1 h*$^+$ *ts-ura4*$^+$ *leu1-32 ura4D18 ade6-210* were gifts from K. Nasmyth. Strains PY614: *h*^{90} *swi6::kanr leu1 ade6-M216*, PY627: *h*^{90} *psc3-GFP-kanr ura4-D18 leu1 ade6-M210*, and PY626: *h*^{90} *psc3-GFP-kanr swi6::ura4*$^+$ *ura4-D18 leu1 ade6-M210* were gifts from Y. Watanabe. Strains 7005: *h*$^+$ *dcr1::NATMX6 otr1R(Sph):ade6*$^+$ *ade6-210 ura4-D18,* 8061: *h*$^+$ *ago1:ura4 otr1R(Sph):ade6*$^+$ *ura4-D18 leu1-32 ade6-M210*, and 2231: *h*$^-$ *ade6-210 leu1-32 ura4-D18 ars1(MIal):pREP42X-GFPswi6-ura4*$^+$ were kindly provided by R. Allshire. We also thank M. Yanagida for strain *h*$^-$ *leu1 mis4-GFP-LEU2*$^+$. Growth conditions and all genetic manipulations were carried out as described previously (Moreno et al., 1991). Cells were grown at 32°C in rich (YES), minimal (EMM), or glycerol (EMM, 0.1% glucose, 3% glycerol) media. Temperature blocks were done at 36°C. Gene expression, driven by *nmt1* or *nmt2* promoter, was repressed by addition of 10 μM thiamine to medium. Cell-cycle arrest conditions are described in Supplemental Experimental Procedures.

Cell-Cycle Arrest

Three different methods were employed to arrest cells.

(1) *Cdc25* and *cdc10* ts cells were grown at 25°C until early exponential phase. Cells were than shifted to restrictive conditions at 36°C for 2.5 hr to block cells in G2 and G1.
(2) Hydroxyurea was used to block cells in early S phase. Exponential cell culture was treated by 11 mM HU for 4 hr, washed, and grown in glycerol medium lacking HU for the next 3 hr to generate a G2 cell population.
(3) WT cells and mutant *rad21-K1* cells were grown in EMM-N at 25°C to block them in G1 phase; this was followed by addition of EMM medium and shift to 36°C to allow G2 phase growth.

For FACS analysis, 1.5 ml aliquots were fixed in 70% ethanol and stored at 4°C. After washing in 50 mM Na-citrate, they were resuspended in 50 mM Na-citrate solution containing 100 mg/ml RNase A and incubated at 37°C for 2 hr, followed by DNA staining with 500 ng/ml propidium iodide. Cell DNA content was measured using the FACScan system with CellQuest software (Becton Dickinson, Franklin Lakes, NJ, USA).

Chromatin Immunoprecipitation

ChIP analysis was performed using standard procedures, and the exact method with our minor modifications is described in Supplemental Experimental Procedures. Purified chromatin was used as template and quantified by using real-time PCR with SYBR Green dye and Rotor-Gene 6 software. Various primer pairs were used to analyze different regions of interest. (Table S1 shows ChIP primers that were employed.)

RNA Isolation and RT-PCR

Total cell RNA from *S. pombe* cells in exponential phase was isolated using Trizol (GIBCO). RNA was dissolved in sterile water and treated with RNase-free DNase (Promega) for 30 min at 37°C. One microgram of total RNA was reverse transcribed using Superscript III system (Invitrogen) with oligo dT_{15} or specific primers (see Table S1). cDNA was diluted to 100 μl in TE buffer and 10 μl was used for PCR. Genomic DNA was employed as a positive control for primer pair efficiency. Results were quantified by using real-time PCR with SYBR Green dye and Rotor-Gene 6 software.

3′RACE analysis has been performed as above, except phased oligo dT was used for RT-PCR. cDNA was amplified with primers in gene ORFs. Amplified DNA was used as template for the second round of PCR with nested primers (see Table S1).

Transcription Run on

Transcription run on analysis was as described previously (Birse et al., 1997) and is described in detail in Supplemental Experimental Procedures.

SUPPLEMENTAL DATA

Supplemental Data include Experimental Procedures, four figures, and one table and can be found with this article online at http://www.cell.com/cgi/content/full/132/6/983/DC1/.

ACKNOWLEDGMENTS

We are grateful to Kim Nasmyth for encouragement and the provision of strains. Thanks also to Chris Norbury, Robin Allshire, Yoshinori Watanabe, and Mitsuhiro Yanagida for additional strains. We are grateful to all members of our lab for valuable advice and discussion, especially Hannah Mischo. We finally thank Chris Norbury and Shona Murphy for advice on the manuscript. This work was supported by a programme grant to N.J.P. from the Wellcome Trust.

Received: July 3, 2007
Revised: November 21, 2007
Accepted: February 5, 2008
Published: March 20, 2008

REFERENCES

Aranda, A., and Proudfoot, N.J. (1999). Definition of transcriptional pause elements in fission yeast. Mol. Cell. Biol. *19*, 1251–1261.

Bahler, J. (2005). Cell-cycle control of gene expression in budding and fission yeast. Annu. Rev. Genet. *39*, 69–94.

Bernard, P., Schmidt, C.K., Vaur, S., Dheur, S., Drogat, J., Genier, S., Ekwall, K., Uhlmann, F., and Javerzat, J.P. (2008). Cell-cycle regulation of cohesin stability along fission yeast chromosomes. EMBO J. *27*, 111–121.

Birse, C.E., Lee, B.A., Hansen, K., and Proudfoot, N.J. (1997). Transcriptional termination signals for RNA polymerase II in fission yeast. EMBO J. *16*, 3633–3643.

Camblong, J., Iglesias, N., Fickentscher, C., Dieppois, G., and Stutz, F. (2007). Antisense RNA stabilization induces transcriptional gene silencing via histone deacetylation in *S. cerevisiae*. Cell *131*, 706–717.

Chen, E.S., Zhang, K., Nicolas, E., Cam, H.P., Zofall, M., and Grewal, S.I. (2008). Cell cycle control of centromeric repeat transcription and heterochromatin assembly. Nature *451*, 734–737.

Chen, S., Reger, R., Miller, C., and Hyman, L.E. (1996). Transcriptional terminators of RNA polymerase II are associated with yeast replication origins. Nucleic Acids Res. *24*, 2885–2893.

Ciosk, R., Shirayama, M., Shevchenko, A., Tanaka, T., Toth, A., Shevchenko, A., and Nasmyth, K. (2000). Cohesin's binding to chromosomes depends on a separate complex consisting of Scc2 and Scc4 proteins. Mol. Cell *5*, 243–254.

Glynn, E.F., Megee, P.C., Yu, H.G., Mistrot, C., Unal, E., Koshland, D.E., DeRisi, J.L., and Gerton, J.L. (2004). Genome-wide mapping of the cohesin complex in the yeast Saccharomyces cerevisiae. PLoS Biol. *2*, E259. 10.1371/journal.pbio.0020259.

Greger, I.H., Aranda, A., and Proudfoot, N. (2000). Balancing transcriptional interference and initiation on the GAL7 promoter of Saccharomyces cerevisiae. Proc. Natl. Acad. Sci. USA *97*, 8415–8420.

Haering, C.H., Lowe, J., Hochwagen, A., and Nasmyth, K. (2002). Molecular architecture of SMC proteins and the yeast cohesin complex. Mol. Cell *9*, 773–788.

Hansen, K., Birse, C.E., and Proudfoot, N.J. (1998). Nascent transcription from the nmt1 and nmt2 genes of Schizosaccharomyces pombe overlaps neighbouring genes. EMBO J. *17*, 3066–3077.

Hegemann, J.H., and Fleig, U.N. (1993). The centromere of budding yeast. Bioessays *15*, 451–460.

Herr, A.J., Jensen, M.B., Dalmay, T., and Baulcombe, D.C. (2005). RNA polymerase IV directs silencing of endogenous DNA. Science *308*, 118–120.

Hirano, T. (2006). At the heart of the chromosome: SMC proteins in action. Nat. Rev. Mol. Cell Biol. *7*, 311–322.

Hongay, C.F., Grisafi, P.L., Galitski, T., and Fink, G.R. (2006). Antisense transcription controls cell fate in *Saccharomyces cerevisiae*. Cell *127*, 735–745.

Lengronne, A., Katou, Y., Mori, S., Yokobayashi, S., Kelly, G.P., Itoh, T., Watanabe, Y., Shirahige, K., and Uhlmann, F. (2004). Cohesin relocation from sites of chromosomal loading to places of convergent transcription. Nature *430*, 573–578.

Martin, A.M., Pouchnik, D.J., Walker, J.L., and Wyrick, J.J. (2004). Redundant roles for histone H3 N-terminal lysine residues in subtelomeric gene repression in Saccharomyces cerevisiae. Genetics *167*, 1123–1132.

Moreno, S., Klar, A., and Nurse, P. (1991). Molecular genetic analysis of fission yeast Schizosaccharomyces pombe. Methods Enzymol. *194*, 795–823.

Motamedi, M.R., Verdel, A., Colmenares, S.U., Gerber, S.A., Gygi, S.P., and Moazed, D. (2004). Two RNAi complexes, RITS and RDRC, physically interact and localize to noncoding centromeric RNAs. Cell *119*, 789–802.

Nasmyth, K., and Haering, C.H. (2005). The structure and function of SMC and kleisin complexes. Annu. Rev. Biochem. *74*, 595–648.

Nonaka, N., Kitajima, T., Yokobayashi, S., Xiao, G., Yamamoto, M., Grewal, S.I., and Watanabe, Y. (2002). Recruitment of cohesin to heterochromatic regions by Swi6/HP1 in fission yeast. Nat. Cell Biol. *4*, 89–93.

Prescott, E.M., and Proudfoot, N.J. (2002). Transcriptional collision between convergent genes in budding yeast. Proc. Natl. Acad. Sci. USA *99*, 8796–8801.

Proudfoot, N., and Gullerova, M. (2007). Gene silencing CUTs both ways. Cell *131*, 649–651.

Proudfoot, N.J., Furger, A., and Dye, M.J. (2002). Integrating mRNA processing with transcription. Cell *108*, 501–512.

Shearwin, K.E., Callen, B.P., and Egan, J.B. (2005). Transcriptional interference–a crash course. Trends Genet. *21*, 339–345.

Tanaka, T., Cosma, M.P., Wirth, K., and Nasmyth, K. (1999). Identification of cohesin association sites at centromeres and along chromosome arms. Cell *98*, 847–858.

Tomonaga, T., Nagao, K., Kawasaki, Y., Furuya, K., Murakami, A., Morishita, J., Yuasa, T., Sutani, T., Kearsey, S.E., Uhlmann, F., et al. (2000). Characterization of fission yeast cohesin: essential anaphase proteolysis of Rad21 phosphorylated in the S phase. Genes Dev. *14*, 2757–2770.

Verdel, A., and Moazed, D. (2005). RNAi-directed assembly of heterochromatin in fission yeast. FEBS Lett. *579*, 5872–5878.

Volpe, T.A., Kidner, C., Hall, I.M., Teng, G., Grewal, S.I., and Martienssen, R.A. (2002). Regulation of heterochromatic silencing and histone H3 lysine-9 methylation by RNAi. Science *297*, 1833–1837.

Zhao, J., Hyman, L., and Moore, C. (1999). Formation of mRNA 3′ ends in eukaryotes: mechanism, regulation, and interrelationships with other steps in mRNA synthesis. Microbiol. Mol. Biol. Rev. *63*, 405–445.